

Article

Multi-Layer Graphene Oxide in Human Keratinocytes: Time-Dependent Cytotoxicity, Proliferation, and Gene Expression

Beatriz Salesa  and Ángel Serrano-Aroca * 

Biomaterials and Bioengineering Lab, Centro de Investigación Traslacional San Alberto Magno, Universidad Católica de Valencia San Vicente Mártir, c/Guillem de Castro 94, 46001 Valencia, Spain; beatriz.salesa@ucv.es

* Correspondence: angel.serrano@ucv.es

Abstract: Few-layer graphene oxide (GO) has shown no or very weak cytotoxicity and anti-proliferative effects in a wide range of cell lines, such as glioma cells and human skin HaCaT cells at concentrations up to 100 $\mu\text{g}/\text{mL}$. However, as multi-layer GO has hardly been explored in the biomedical field, in this study, this other type of GO was examined in human keratinocyte HaCaT cells treated with different concentrations, ranging from 0.01 to 150 $\mu\text{g}/\text{mL}$, for different periods of time (3, 12, and 24 h). The results revealed a time–concentration dependence with two non-cytotoxic concentrations (0.01 and 0.05 $\mu\text{g}/\text{mL}$) and a median effective concentration value of 4.087 $\mu\text{g}/\text{mL}$ at 24 h GO exposure. Contrary to what has previously been reported for few-layer GO, cell proliferation of the HaCaT cells in contact with the multi-layer GO at 0.01 $\mu\text{g}/\text{mL}$ showed identical proliferative activity to an epidermal growth factor (1.6-fold greater than the control group) after 96 h. The effects of the multi-layer GO on the expression of 13 genes (SOD1, CAT, MMP1, TGFB1, GPX1, FN1, HAS2, LAMB1, LUM, CDH1, COL4A1, FBN, and VCAN) at non-cytotoxic concentrations of GO in the HaCaT cells were analyzed after 24 h. The lowest non-cytotoxic GO concentration was able to upregulate the CAT, TGFB1, FN1, and CDH1 genes, which confirms multi-layer GO's great potential in the biomedical field.

Keywords: graphene oxide; human keratinocytes; proliferation; gene expression; cytotoxicity



Citation: Salesa, B.; Serrano-Aroca, Á. Multi-Layer Graphene Oxide in Human Keratinocytes: Time-Dependent Cytotoxicity, Proliferation, and Gene Expression. *Coatings* **2021**, *11*, 414. <https://doi.org/10.3390/coatings11040414>

Academic Editor: Xiangsheng Liu

Received: 6 March 2021

Accepted: 31 March 2021

Published: 2 April 2021

Publisher's Note: MDPI stays neutral with regard to jurisdictional claims in published maps and institutional affiliations.



Copyright: © 2021 by the authors. Licensee MDPI, Basel, Switzerland. This article is an open access article distributed under the terms and conditions of the Creative Commons Attribution (CC BY) license (<https://creativecommons.org/licenses/by/4.0/>).

1. Introduction

Graphene oxide (GO) nanosheets are two-dimensional carbon-based nanomaterials (CBNs) with a high surface/volume ratio. The oxygenated functional groups (hydroxyls, carbonyls, and epoxy groups) located at the edges and basal planes of the GO nanosheets, render them easily dispersible in polar solvents [1,2]. These CBNs present great potential in the biomedical field due to their excellent mechanical performance and unique biological properties, such as antimicrobial activity, which make them promising for a wide range of potential industrial applications [3,4]. CBNs possess unique qualities, such as broad-spectrum antimicrobial properties capable of inactivating Gram-positive and Gram-negative bacteria, fungi, and viruses, including enveloped RNA viruses such as SARS-CoV-2 [3,5,6]. CBNs' antimicrobial action mechanisms, such as those of graphene oxide, are usually attributed to a combination of several physical and chemical mechanisms different from those observed in conventional compounds and associated with a low risk of inducing microbial resistance: entrapment of microorganisms, membrane disruption, transfer of electrons, and the induction of oxidative stress by reactive oxygen species (ROS) [7,8]. Furthermore, CBNs are biocompatible, biodegradable, able to induce tissue regeneration, and could provide long-lasting solutions in microbiology due to their mechanisms of action [9–12]. Since bacterial pathogenic strains such as *Streptococcus pneumoniae* and fungal pathogens may contribute to SARS-CoV-2-mediated pneumonia, among many other CBNs, GO have been proposed as next-generation antiviral agents to treat the coronavirus disease 2019 (COVID-19) [5]. From CBN types such as graphene, graphene oxide,

fullerene, carbon dots, carbon nanotubes, and many others, multiple variants of GO have been synthesized and studied, including few-layer nanosheets, multi-layer nanosheets, dots, nanocaps, flakes, and nanoribbons or nanotubes, among many other forms [13,14]. Few-layer GO has shown no or low cytotoxicity in human A549 lung epithelial cells [15] and in human keratinocyte HaCaT cells [16]. Single-layer GO showed lower toxicity in glioma cells than its reduced form (reduced GO) [17]. Single-layer GO showed low toxicity in NIH-3T3 fibroblast cells [18], and single- or two-layer GO in human lung fibroblast (HLF) cells assessed with methyl thiazolyl tetrazolium showed no cytotoxicity at 10 µg/mL after 24 h [19], nor did a few-layer GO dose of less than 20 µg/mL exhibit toxicity in human fibroblast cells [9]. In the same line of research, monolayer GO has shown a lesser effect than multi-GO on cell viability in DC2.4 dendritic cells [20]. This study showed that both mono-GO and multi-GO significantly induced the generation of reactive oxygen species in the DC2.4 cells. However, another study performed with one-layer GO and four-layer GO showed similar cytotoxicity in human Caucasian breast adenocarcinoma MCF7 cells after 48 h of exposure [21], so further investigation is necessary for a better understanding of GO cytotoxicity. Furthermore, a previous study of few-layer GO showed anti-proliferative capacity in human keratinocyte HaCaT cells and glioma cells [16,17]. However, as many other reports in the literature have given controversial results on GO cytotoxicity, further research is needed. The use of pure, few-layer GO, or the composite material combined with other compounds, thus shows great proliferative potential in a wide variety of cell lines [22–25].

Even though it is still not clearly understood, single-layer GO, multi-layer GO, and GO in the form of nanoribbons have been shown to affect gene expression [13,26,27].

In this study, the time-dependent cytotoxicity and proliferative activity of multi-layer GO (>10 layers) were analyzed in human keratinocyte HaCaT cells, together with the capacity of multi-layer GO to upregulate genes associated with oxidative stress, the extracellular matrix, and the synthesis of proteins associated with the maintenance and repair of different tissues. This study thus focuses on better understanding the ways in which this multi-layer nanomaterial affects not only cell toxicity but also its benefits when used at low, non-cytotoxic concentrations in terms of proliferative capacity and modifications of gene expression.

2. Materials and Methods

2.1. Materials

Graphene oxide nanosheets (GO, 15–20 sheets, 4–10% edge-oxidized, Sigma-Aldrich, St Louis, MO, USA) were used as received. This GO was previously characterized [28] and classified according to the number of graphene layers, average lateral size, and carbon-to-oxygen (C/O) atomic ratio determined by Raman spectroscopy and high-resolution electron microscopy equipped with energy-dispersive X-ray spectroscopy according to the GRAPHENE Flagship Project of the European Union for the unequivocal classification of these materials [29]. The results of this characterization thus showed a G peak intensity/2D peak intensity (I_{2D}/I_G) ratio of 0.87, which corresponds to a number of GO layers >10, in good agreement with the product information provided by the manufacturer (Sigma-Aldrich). The 2D GO nanosheets possessed an average lateral dimension of 153.8 ± 57.2 nm and a C/O ratio of 15.4. The zeta potential of these GO nanosheets was analyzed in methanol/water solutions ranging from 2 to 50% *w/w* methanol on a Zetasizer Nanoseries from Malvern Instruments by de Oliveira et al. [30]. The results of this analysis showed that this multi-layer GO had a surface charge ranging from -26.52 ± 1.44 to -28.94 ± 3.45 ζ/mV. The dynamic light scattering (DLS) technique was used to evaluate the particle hydrodynamic size of these GO nanosheets by Agilar et al. [31]. The particle size values ranged from 300 to 500 nm, depending on the nanofluid (prepared with polyethylene glycol, 1-octadecanethiol, or Triton X-100 surfactant) used for these measurements.

2.2. Cytotoxicity Assay

The cytotoxicity of different compounds was evaluated against the human keratinocyte HaCaT cell line, which was provided by the La Fe Research Institute and Hospital, using a 3-(4, 5-dimethylthiazol-2-yl)-2, 5-diphenyl tetrazolium (MTT) assay. First of all, 10,000 cells per well, resuspended in low-glucose Dulbecco's modified Eagle medium (DMEM) supplemented with 10% fetal bovine serum (FBS), 5% penicillin–streptomycin, and 5% glutamine, were seeded in 96-micro-well plates and grown for 24 h at 37 °C in a humidified atmosphere of 5% CO₂ in an incubator. The culture medium was subsequently aspirated and replaced with 100 µL of medium containing several concentrations of GO (0.01, 0.05, 0.1, 0.5, 1, 5, 10, 20, 40, 80, and 150 µg/mL). Stock solutions of nanomaterials were prepared in sterile low-glucose DMEM without FBS, supplemented with glutamine and antibiotics, and were sonicated for 2 h, after which the solutions were immediately prepared and dispensed to the cell culture. For each GO concentration, cells were incubated separately for different periods of time to evaluate cytotoxicity at 3, 12, and 24 h. Six replicate samples were prepared in wells for each concentration. An untreated control was also run simultaneously under identical conditions. After incubation, the medium was replaced with MTT reagent, incubated under the same conditions as the culture, and then formazan crystals were solubilized with DMSO. Cell viability was determined based on the absorbance at 550 nm, using a Varioskan microplate reader (Thermo Fisher, Waltham, MA, USA). To avoid false positives due to cell pigmentation with GO from concentration 80 µg/mL onwards, the same experiment was carried out in parallel, excluding the addition of the MTT reagent. The background color was thus subtracted from the final result.

2.3. Proliferation Assay

In order to study the potential proliferation effect of GO in the HaCaT cell line, two non-toxic concentrations were chosen based on the cytotoxicity assay results to ensure no increase in cytotoxicity when increasing the exposure time to 96 h. Cells were seeded in a 96-well culture plate (5×10^3) and a stock solution was prepared, following the same protocol as in the cytotoxicity assay, with the exception of changing DMEM without FBS for DMEM with 0.5% FBS. Cells were cultured at 37 °C in a humidified atmosphere of 5% CO₂ in the incubator for 72 and 96 h. A positive control was included, treating the HaCaT cells with epidermal growth factor (EGF) at 15 ng/mL. Cell proliferation was measured using the MTT assay, following the same procedure as in the cytotoxicity assay.

2.4. Gene Expression

Gene expression analysis was performed with the human keratinocyte cell line HaCaT seeded in a 6-well culture plate at a density of 1.5×10^5 cells per well. Based on the cytotoxicity results, two non-toxic concentrations were chosen at 24 h to perform this assay. Stock solutions were prepared following the protocol described for the cytotoxicity and proliferation tests. After the cells had been left for 24 h with the compounds, the supernatant was aspirated and the cells were washed twice with PBS (1×) to remove any trace of the treatment. The extraction buffer was immediately added to each well and the plates were frozen in liquid nitrogen and preserved at −80 °C until RNA extraction. Each condition was tested in triplicate. RNA was isolated using an RNA purification kit (Norgen, Thorold, ON, Canada) according to the manufacturer's protocol. Quality and concentrations of each sample were measured using a Nanodrop™ One (Thermo Scientific™, Dreieich, Germany), and cDNA was synthesized using Prime Script™ RT Reagent Kit (Perfect Real Time) (Takara Bio Inc., Shiga, Japan). For the quantitative real-time PCR (qPCR), TB Green Premix Ex Taq (Takara Bio Inc.) was used, following the manufacturer's protocol in a 384 QuantStudio 5 (Thermo Scientific™, Dreieich, Germany). Data were analyzed by QuantStudio™ Design & Analysis Software v2 (Thermo Fisher, Waltham, MA, USA). The primers for amplification of fourteen target genes and a reference gene (β -actin/ACTB) were determined using Primer-Blast software (available at: <http://www.ncbi.nlm.nih.gov/tools/primer-blast>)

(accessed on 1 April 2021)). Data were normalized according to the expression of the reference gene. All the primers used are listed in Table 1.

Table 1. Details of gene-specific used in RT-qPCR assay.

Gene Symbol (Access Number)	Gene Name	Oligo Sequences	Function
ACTB (NM_001101)	Actin beta	5'-CCATGCCACCATCACGC-3' 5'-CACAGAGCCTCGCCTTG-3'	Highly conserved protein that is involved in cell motility, structure, and integrity.
CAT (NM_001752)	Catalase	5'-TGAATGAGGAACAGAGAAACG-3' 5'-AGATCCGGACTGCACAAAG-3'	Encodes catalase, a key antioxidant enzyme in the body's defense against oxidative stress.
MMP1 (NM_001145938)	Matrix metalloproteinase 1	5'-GGACCATGCCATTGAGAAAG-3' 5'-TCCTCCAGGTCCATCAAAAG-3'	Involved in the breakdown of extracellular matrix in normal physiological processes.
GPX1 (NM_000581)	Glutathione peroxidase 1	5'-TTGGGCATCAGGAGAACGC-3' 5'-ACCGTTCACCTCCCACTTC-3'	Catalyzes the reduction of organic hydroperoxides and hydrogen peroxide by glutathione and thereby protects cells against oxidative damage.
COL4A1 (NM_000088)	Collagen type I alpha 1	5'-CAAGGGCAGCAGAGTTTGC-3' 5'-AAAATCCACAGGCTCCCC-3'	Abundant in bone, cornea, dermis, and tendon. Mutations in this gene are associated with osteogenesis imperfect types I-IV.
TGFB1 (NM_000660)	Transforming growth factor beta 1	5'-AGCTGTACATTGACTTCCGCA-3' 5'-TGTCAGGCTCCAAATGATAGG-3'	Regulates cell proliferation, differentiation, and growth.
HAS2 (NM_005328)	Hyaluronan synthase 2	5'-CCGAGAATGGCTGTACAATGC-3' 5'-AGAGCTGGATTACTGTGGCAA-3'	Serves a variety of functions, including space filling, lubrication of joints, and provision of a matrix through which cells can migrate.
LAMB1 (NM_002291)	Laminin subunit beta 1	5'-CAGGGTGTGAGTCAAGGAA-3' 5'-TGTGTCTCGCTGAGGGTGT-3'	Implicated in a wide variety of biological processes, including cell adhesion, differentiation, migration, signaling, neurite outgrowth, and metastasis.
LUM (NM_002345)	Lumican	5'-ACTTGGTAGCTTTCAGGCA-3' 5'-TTCTCGCATGATTGGTGGT-3'	The major keratan sulfate proteoglycan of the cornea, but is also distributed in interstitial collagenous matrices throughout the body.
FN1 (NM_001306129)	Fibronectin 1	5'-GGCCAGTCTACAACCAAGT-3' 5'-CGGGAATCTCTCTGTGACG-3'	Involved in cell adhesion and migration processes, including embryogenesis, wound healing, blood coagulation, host defense, and metastasis.
VCAN (NM_001126336)	Versican	5'-CTGGTCTCCGCTGTATCCTG-3' 5'-ATCGCTGCAAAATGAACCCG-3'	Involved in cell adhesion, proliferation, migration, and angiogenesis, and plays a central role in tissue morphogenesis and maintenance.
CDH1 (NM_001317184)	Cadherin 1	5'-AACAGCAGCTACACAGCCCT-3' 5'-TCTGGTATGGGGCGGTGTC-3'	Loss of function of this gene is thought to contribute to cancer progression by increasing proliferation, invasion, and/or metastasis.
FBN (NM_000138)	Fibrillin 1	5'-ATCCAACACGTCATCAGT-3' 5'-AGAGCGGTATCAACACAGC-3'	Extracellular matrix glycoprotein that serves as a structural component of calcium-binding microfibrils, providing force-bearing structural support in elastic and nonelastic connective tissue throughout the body.
SOD1 (NM_000454)	Superoxide dismutase 1	5'-GGTGTGCCGATGTGCT-3' 5'-TCCACCTTGTCCCAAGTCA-3'	The protein encoded by this gene binds copper and zinc ions and is one of two isozymes responsible for destroying free superoxide radicals in the body.

2.5. Statistical Analysis

The results obtained in this study were statistically analyzed by ANOVA, followed by multiple Tukey's post-hoc analysis. Median effective concentration (EC₅₀) values were estimated using Probit analysis. Results were obtained on GraphPad Prism 6 software at a significance level of at least $p < 0.05$.

3. Results and Discussion

The time-dependent cytotoxicity, proliferation, and gene expression results determined for multi-layer GO in human keratinocyte HaCaT cells are presented in the following subsections.

3.1. Cytotoxicity Assay

The cytotoxic effects of multi-layer GO were examined in HaCaT cells treated with different concentrations ranging from 0.01 to 150 µg/mL for different periods of time (3, 12, and 24 h). At 3 h of treatment, as only the highest concentration (150 µg/mL) was slightly toxic for the cell line (survival up to 75%), the mean effective concentration (EC₅₀) for this time could not be determined due to the lack of toxicity above 50%. However, the increased GO concentration and time exposure showed a negative correlation with the survival rate of the cells, which indicated dose-dependent cytotoxicity (Figure 1).

EC₅₀ at 24 h was lower than at 12 h, indicating that GO toxicity increases with treatment time (Table 2).

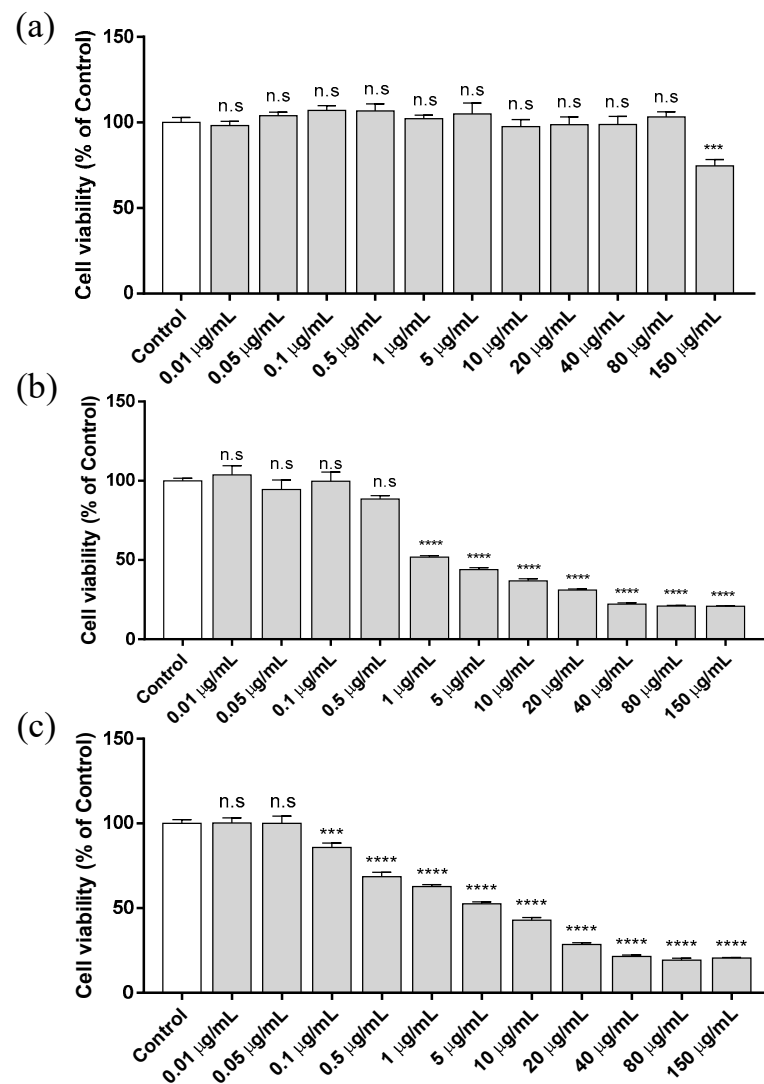


Figure 1. Cell viability in human keratinocyte HaCaT cells, after 3 (a), 12 (b), and 24 (c) h of exposure to different concentrations of graphene oxide (GO) ranging from 0.01 to 150 µg/mL. Cell viability was evaluated by the 3-(4, 5-dimethylthiazol-2-yl)-2, 5-diphenyl tetrazolium (MTT) assay. Results are represented as a percentage of the control group. Data are presented as the mean ± standard error of six replicates. The ANOVA results of the different GO concentrations with respect to control are indicated in the plot. *** $p > 0.01$; **** $p > 0.001$; n.s: not significant.

Table 2. Mean effective concentration (EC_{50}) of HaCaT cells after treatment with graphene oxide (GO) at different exposure times. Mean EC_{50} and 95% confidence intervals (CI) are shown as the mass–volume concentration, µg/mL. Goodness of fit (R square) is also indicated.

GO Exposure	EC_{50} (µg/mL)	95% CI	R Square
12 h	5.615	4.302–7.237	0.9045
24 h	4.087	3.335–5.013	0.9396

This type of multi-layer GO with more than 10 layers was more toxic than other few-layer GO types studied previously in murine NIH-3T3 fibroblasts, U87 and U118 glioma cells, human lung fibroblast cells, and even human skin HaCaT cells, up to 100 µg/mL [9,16–19]. These results are in good agreement with previous studies, such as that by Yang et al. [20],

in which multi-GO showed greater toxicity towards cell viability than mono-GO in DC2.4 dendritic cells.

3.2. Proliferation Assay

The potential proliferation effect of multi-layer GO in the HaCaT cell line was studied using two non-toxic concentrations (0.01 and 0.005 $\mu\text{g}/\text{mL}$) based on the lowest non-cytotoxic concentration (Figure 1) to avoid cytotoxicity by increasing the time of exposure to 72 and 96 h (Figure 2).

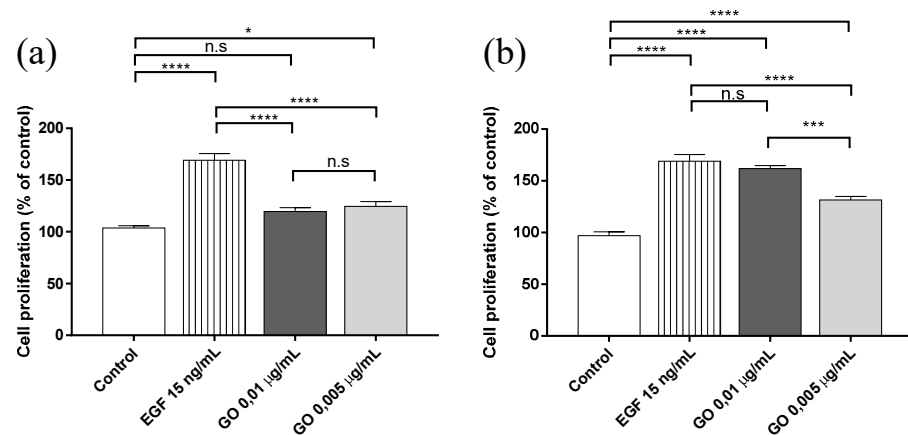


Figure 2. Proliferation in human keratinocytes stimulated by exposure to GO for 72 (a) and 96 (b) h. Data are presented as the mean \pm standard error of the mean (SEM) of six replicates. The ANOVA results of the different graphene oxide (GO) concentrations and epidermal growth factor (EGF) are indicated in the plot with respect to control. * $p > 0.05$; *** $p > 0.01$; **** $p > 0.001$; n.s: not significant.

Contact lasting 72 h with the multi-layer GO was not long enough to induce a significant proliferative effect. Only a slight significant increase was observed at the highest non-cytotoxic GO concentration of 0.005 $\mu\text{g}/\text{mL}$ with respect to the control group. However, the cell proliferation achieved after exposure of 96 h with the GO compound at 0.01 $\mu\text{g}/\text{mL}$ was practically identical to that obtained with the epidermal growth factor, showing that cell proliferation at this low concentration of multi-layer GO was 1.6-fold greater than in the control group after this longer period of time (96 h). However, as few-layer GO has shown anti-proliferative activity in the same cell line, in human skin HaCaT cells and in glioma cells [16,17], the proliferative effect achieved in these experiments could be attributed to the multi-layer form of the GO (>10 layers) used in the present study. However, the mechanism behind this change in proliferation between multi-layer and few-layer is unclear since many controversial results have been published in this regard. Scaffolds produced with single-layer GO showed stimulative cell proliferation in mouse osteoblastic MC3T3-E1 cells in a significant and dose-dependent manner [22]. Few-layer GO alone [23] or in combination with other materials such as black phosphorus [24] or chitosan [25] has shown good potential for proliferative activity in colorectal adenocarcinoma HT-29 cells, osteoblasts, and human mesenchymal stem cells, respectively. Although there is still uncertainty regarding the biological properties of graphene oxide and the added problems that can occur in a multitude of forms, this carbon nanomaterial has shown great potential in a wide range of biological applications; however, it is still necessary to elucidate its biofunctionalization and standardization according to the number of layers, chemical characteristics, and sizes.

3.3. Gene Expression

To determine the activation or inhibition of different metabolic routes (oxidative stress, the extracellular matrix, and the synthesis of proteins related to the maintenance and repair of different tissues) due to the exposure of GO in human keratinocyte HaCaT cells, the

expression levels of the different genes (Table 1) involved were analyzed. Figure 3 shows the effect of multi-layer GO on the expression of 13 genes (SOD1, CAT, MMP1, TGFB1, GPX1, FN1, HAS2, LAMB1, LUM, CDH1, COL4A1, FBN, and VCAN) at non-cytotoxic concentrations (0.01 and 0.05 $\mu\text{g}/\text{mL}$) in HaCaT cells after 24 h.

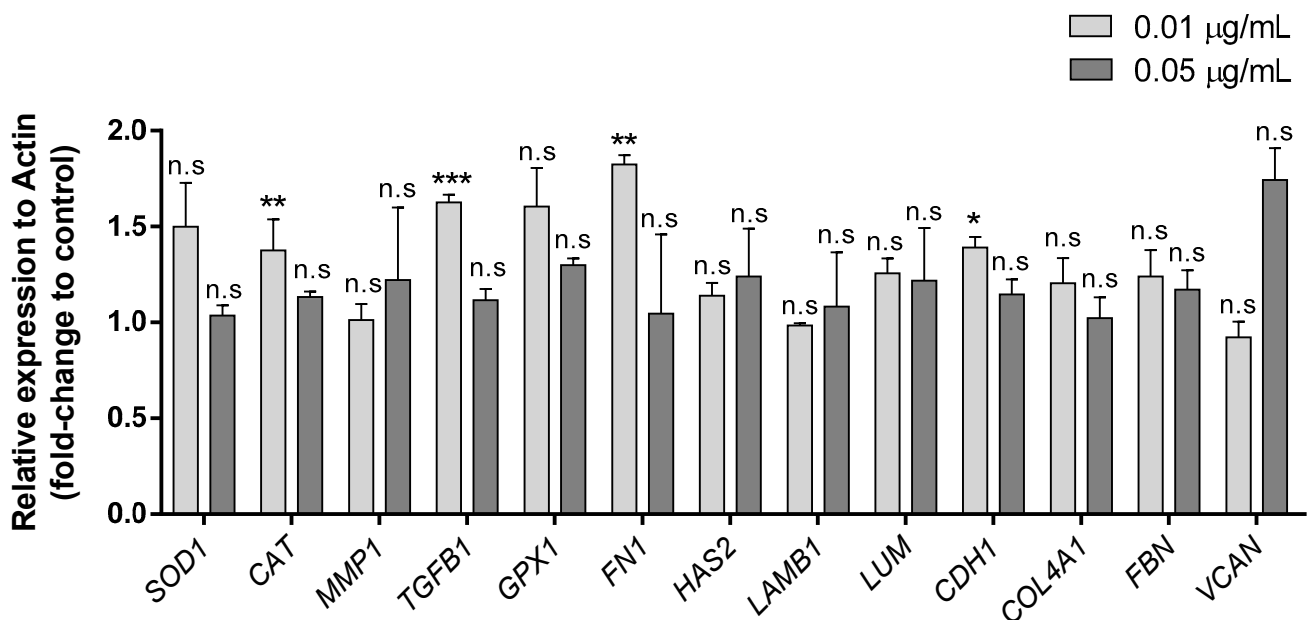


Figure 3. Effect of multi-layer GO on the expression of 13 genes (SOD1, CAT, MMP1, TGFB1, GPX1, FN1, HAS2, LAMB1, LUM, CDH1, COL4A1, FBN, and VCAN) at non-cytotoxic concentrations (0.01 and 0.05 $\mu\text{g}/\text{mL}$) in the human keratinocyte HaCaT cell line after 24 h. Data are presented as mean \pm SEM from three replicate measurements. Results are represented as fold-change of control and relative expression to ACTB. (* $p < 0.05$; ** $p < 0.01$; *** $p < 0.001$, n.s: not significant).

The study results show that exposure to GO for 24 h did not produce any effect on human keratinocyte HaCaT cells at the highest concentration (0.05 $\mu\text{g}/\text{mL}$). This could be attributed to the fact that this concentration is close to the cytotoxic level (0.1 $\mu\text{g}/\text{mL}$) determined in this study. However, the lowest non-cytotoxic concentration (0.01 $\mu\text{g}/\text{mL}$) induced the upregulation of four (CAT, TGFB1, FN1 and CDH1) of the 13 genes analyzed. From the catalase (CAT) and the glutathione per-oxidase 1 (GPX1) genes, which code for the synthesis of enzymes involved in the neutralization of H_2O_2 , acting as importer antioxidants, only CAT was upregulated at the lowest concentration after 24 h of exposure. The activation of these genes has been associated with important defense mechanisms against stressors in different types of skin cells during human skin photoaging processes [32–34]. Other researchers found upregulation of these two genes in HaCaT cells treated with caffeic acid or ferulic acid to have a protective effect on cells from UVA radiation [35], although the required amount of these two compounds was much higher (7.5–30 $\mu\text{g}/\text{mL}$).

The low concentration exposure of GO in the HaCaT cells also increased the expression of TGFB1, which regulates cell proliferation, differentiation, and growth [36,37], and the FN1 involved in cell adhesion and migration processes [38]. Among the wide range of effects of TGF- β ligands, TGF- β 1 enhances differentiation toward chondrocytes, consistent with their independent identification and purification as cartilage-inducing factors A [39]. On the other hand, fibronectin is one of the extracellular matrix components that controls cell proliferation, to which cells adhere via the integrin family of transmembrane receptors [40]. These results are in good agreement with the proliferation results shown in Figure 2 and with a recent study published by our group [11], in which the incorporation of a low percentage of multi-layer GO in the biopolymer poly(3-hydroxybutyrate-co-3-hydroxyvalerate) (PHBV) showed improved proliferative activity and enhanced cell adhesion of canine adipose-derived mesenchymal stem cells. The enhancements achieved

with multi-layer GO nanosheets were higher than those achieved with other carbon nanomaterials composed of nanofibers [11].

Of the genes involved in the synthesis of different proteins, only the expression of cadherin 1 (CDH1) was altered. The type I cadherins include transmembrane glycoproteins, vital in the morphogenesis and development of normal animal tissue [41], and cadherin-based adherens junctions have been shown to play a critical role in connecting cells with each other to form tissue. HaCaT cell exposure to GO at 0.01 µg/mL induced the upregulation of the gene involved in the synthesis of this glycoprotein.

The matrix metalloproteinases (MMPs) comprise a family of zinc-containing proteinases responsible for degrading the extracellular matrix proteins produced by skin cells, including fibroblasts and keratinocytes, with clear links to malignancy [42]. It is commonly used to induce the activation of matrix metalloproteinase 1 (MMP1) through solar radiation. However, keratinocytes damaged by other pathways can activate this pathway on their own. Figure 3 shows that MMP1 was not activated by GO exposure, showing that the expression of this gene was not affected by the presence of the nanomaterial in HaCaT cells after 24 h and that no such negative effect can be attributed to this gene. We found no alterations of the expression of the rest of the genes analyzed in this study.

Previous gene expression studies performed with mono-layer GO confirmed its ability to intercalate efficiently into DNA molecules (this being the principal reason for its mutagenic effect [27]) and also to promote ROS generation, resulting in potential DNA damage [43]. In contrast to what has been reported for mono-layer GO, we did not find any negative effects derived from the use of multi-layer GO.

Multi-layer GO presents a time–concentration dependence and can be used at an optimal non-cytotoxic concentration of 0.01 µg/mL, which is able to induce cell proliferation and upregulate CAT, TGFB1, FN1, and CDH1 genes. These results therefore confirm that this type of GO shows great promise in biomedicine and can provide greater benefits than conventional drugs. In addition to its excellent characteristics described here, it possesses broad-spectrum antimicrobial activity [3,5,6], it is biocompatible and biodegradable, it induces tissue regeneration, and it could provide long-lasting biomedical solutions due to its low risk of inducing microbial resistance in biomedical applications [9–12].

4. Conclusions

Multi-layer GO has been shown to be more toxic (≥ 0.1 µg/mL and a median effective concentration value of 4.087 µg/mL at 24 h) than previously reported for few-layer GO in human keratinocyte HaCaT cells. However, even though many controversial results have been reported regarding the proliferative potential of carbon nanomaterials, this multi-layer graphene oxide showed proliferative activity similar to an epidermal growth factor (1.6-fold greater than the control group) after 96 h, in contrast to the anti-proliferative effect of few-layer GO reported for the same cell line and glioma cells.

The gene expression analysis of 13 genes (SOD1, CAT, MMP1, TGFB1, GPX1, FN1, HAS2, LAMB1, LUM, CDH1, COL4A1, FBN, and VCAN) showed that exposure to low, non-cytotoxic concentrations of multi-layer GO (0.01 µg/mL) upregulates the CAT gene, which encodes the antioxidant catalase enzyme against oxidative stress; the TGFB1 gene, which regulates cell proliferation, differentiation, and growth; the FN1 gene, which encodes cell adhesion and migration; and the CDH1 gene, involved in the synthesis of transmembrane glycoproteins, confirming the biomedical potential of this graphene oxide type.

Author Contributions: Conceptualization, methodology, validation, formal analysis, software, investigation, data curation, visualization, writing—original draft preparation: B.S. and Á.S.-A.; resources, supervision, project administration, writing—review and editing, funding acquisition: Á.S.-A. All authors have read and agreed to the published version of the manuscript.

Funding: This research was funded by the Fundación Universidad Católica de Valencia San Vicente Mártir, grant 2020-231-006UCV (awarded to Á.S.-A).

Institutional Review Board Statement: Not applicable.

Informed Consent Statement: Not applicable.

Data Availability Statement: Data are contained within the article.

Conflicts of Interest: The authors declare no conflict of interest.

References

1. Serrano-Aroca, Á.; Iskandar, L.; Deb, S. Green synthetic routes to alginate-graphene oxide composite hydrogels with enhanced physical properties for bioengineering applications. *Eur. Polym. J.* **2018**, *103*, 198–206. [CrossRef]
2. Zhao, J.; Liu, L.; Li, F. *Graphene Oxide: Physics and Applications*; Springer: Berlin/Heidelberg, Germany, 2014.
3. Martí, M.; Frigols, B.; Salesa, B.; Serrano-Aroca, Á. Calcium alginate/graphene oxide films: Reinforced composites able to prevent *Staphylococcus aureus* and methicillin-resistant *Staphylococcus epidermidis* infections with no cytotoxicity for human keratinocyte HaCaT cells. *Eur. Polym. J.* **2019**, *110*, 14–21. [CrossRef]
4. Yu, X.; Zhang, W.; Zhang, P.; Su, Z. Fabrication technologies and sensing applications of graphene-based composite films: Advances and challenges. *Biosens. Bioelectron.* **2017**, *89*, 72–84. [CrossRef]
5. Serrano-Aroca, Á.; Takayama, K.; Tuñón-Molina, A.; Seyran, M.; Hassan, S.S.; Choudhury, P.P.; Uversky, V.N.; Lundstrom, K.; Adadi, P.; Palù, G.; et al. Carbon-based nanomaterials: Promising antiviral agents to combat COVID-19 in the microbial resistant era. *Preprints* **2021**, 2021010297. Available online: <https://www.preprints.org/manuscript/202101.0297/v1> (accessed on 31 March 2021). [CrossRef]
6. Innocenzi, P.; Stagi, L. Carbon-based antiviral nanomaterials: Graphene, C-dots, and fullerenes. A perspective. *Chem. Sci.* **2020**, *11*, 6606–6622. [CrossRef] [PubMed]
7. Zou, X.; Zhang, L.; Wang, Z.; Luo, Y. Mechanisms of the Antimicrobial Activities of Graphene Materials. *J. Am. Chem. Soc.* **2016**, *138*, 2064–2077. [CrossRef] [PubMed]
8. Tegou, E.; Magana, M.; Katsogridaki, A.E.; Ioannidis, A.; Raptis, V.; Jordan, S.; Chatzipanagiotou, S.; Chatzandroulis, S.; Ornelas, C.; Tegos, G.P. Terms of endearment: Bacteria meet graphene nanosurfaces. *Biomaterials* **2016**, *89*, 38–55. [CrossRef] [PubMed]
9. Du, Y.; Ge, J.; Li, Y.; Ma, P.X.; Lei, B. Biomimetic elastomeric, conductive and biodegradable polycitrate-based nanocomposites for guiding myogenic differentiation and skeletal muscle regeneration. *Biomaterials* **2018**, *157*, 40–50. [CrossRef] [PubMed]
10. Tandon, B.; Magaz, A.; Balint, R.; Blaker, J.J.; Cartmell, S.H. Electroactive biomaterials: Vehicles for controlled delivery of therapeutic agents for drug delivery and tissue regeneration. *Adv. Drug Deliv. Rev.* **2018**, *129*, 148–168. [CrossRef]
11. Rivera-Briso, A.L.; Aachmann, F.L.; Moreno-Manzano, V.; Serrano-Aroca, Á. Graphene oxide nanosheets versus carbon nanofibers: Enhancement of physical and biological properties of poly(3-hydroxybutyrate-co-3-hydroxyvalerate) films for biomedical applications. *Int. J. Biol. Macromol.* **2020**, *143*, 1000–1008. [CrossRef]
12. Wu, X.; Ding, S.-J.; Lin, K.; Su, J. A review on the biocompatibility and potential applications of graphene in inducing cell differentiation and tissue regeneration. *J. Mater. Chem. B* **2017**, *5*, 3084–3102. [CrossRef]
13. Ricci, R.; Leite, N.; Da-Silva, N.; Pacheco-Soares, C.; Canevari, R.; Marciano, F.; Webster, T.; Lobo, A. Graphene oxide nanoribbons as nanomaterial for bone regeneration: Effects on cytotoxicity, gene expression and bactericidal effect. *Mater. Sci. Eng. C* **2017**, *78*, 341–348. [CrossRef]
14. Lu, P.; Yazdi, A.Z.; Han, X.X.; Al Husaini, K.; Haime, J.; Waye, N.; Chen, P. Mechanistic Insights into the Cytotoxicity of Graphene Oxide Derivatives in Mammalian Cells. *Chem. Res. Toxicol.* **2020**, *33*, 2247–2260. [CrossRef]
15. A Jasim, D.; Lozano, N.; Kostarelos, K. Synthesis of few-layered, high-purity graphene oxide sheets from different graphite sources for biology. *2D Mater.* **2016**, *3*, 014006. [CrossRef]
16. Pelin, M.; Fusco, L.; León, V.; Martín, C.; Criado, A.; Sosa, S.; Vázquez, E.; Tubaro, A.; Prato, M. Differential cytotoxic effects of graphene and graphene oxide on skin keratinocytes. *Sci. Rep.* **2017**, *7*, 40572. [CrossRef]
17. Jaworski, S.; Sawosz, E.; Kutwin, M.; Wierzbicki, M.; Hinzmann, M.; Grodzik, M.; Winnicka, A.; Lipińska, L.; Wlodyga, K.; Chwalibog, A. In vitro and in vivo effects of graphene oxide and reduced graphene oxide on glioblastoma. *Int. J. Nanomed.* **2015**, *10*, 1585–1596. [CrossRef]
18. Ryoo, S.-R.; Kim, Y.-K.; Kim, M.-H.; Min, D.-H. Behaviors of NIH-3T3 Fibroblasts on Graphene/Carbon Nanotubes: Proliferation, Focal Adhesion, and Gene Transfection Studies. *ACS Nano* **2010**, *4*, 6587–6598. [CrossRef]
19. Wang, A.; Pu, K.; Dong, B.; Liu, Y.; Zhang, L.; Zhang, Z.; Duan, W.; Zhu, Y. Role of surface charge and oxidative stress in cytotoxicity and genotoxicity of graphene oxide towards human lung fibroblast cells. *J. Appl. Toxicol.* **2013**, *33*, 1156–1164. [CrossRef]
20. Yang, Z.; Pan, Y.; Chen, T.; Li, L.; Zou, W.; Liu, D.; Xue, D.; Wang, X.; Lin, G. Cytotoxicity and Immune Dysfunction of Dendritic Cells Caused by Graphene Oxide. *Front. Pharmacol.* **2020**, *11*, 11. [CrossRef]
21. Peruzynska, M.; Cendrowski, K.; Barylak, M.; Tkacz, M.; Piotrowska, K.; Kurzawski, M.; Mijowska, E.; Drozdziak, M. Comparative in vitro study of single and four layer graphene oxide nanoflakes—Cytotoxicity and cellular uptake. *Toxicol. Vitro* **2017**, *41*, 205–213. [CrossRef]
22. Miyaji, H.; Kato, A.; Takita, H.; Iwanaga, T.; Momose, T.; Ogawa, K.; Murakami, S.; Sugaya, T.; Kawanami, M.; Nishida, E. Graphene oxide scaffold accelerates cellular proliferative response and alveolar bone healing of tooth extraction socket. *Int. J. Nanomed.* **2016**, *11*, 2265–2277. [CrossRef] [PubMed]

23. Ruiz, O.N.; Fernando, K.A.S.; Wang, B.; Brown, N.A.; Luo, P.G.; McNamara, N.D.; Vangsnæs, M.; Sun, Y.-P.; Bunker, C.E. Graphene Oxide: A Nonspecific Enhancer of Cellular Growth. *ACS Nano* **2011**, *5*, 8100–8107. [[CrossRef](#)] [[PubMed](#)]
24. Liu, X.; Miller, A.L.; Park, S.; George, M.N.; Waletzki, B.E.; Xu, H.; Terzic, A.; Lu, L. Two-Dimensional Black Phosphorus and Graphene Oxide Nanosheets Synergistically Enhance Cell Proliferation and Osteogenesis on 3D Printed Scaffolds. *ACS Appl. Mater. Interfaces* **2019**, *11*, 23558–23572. [[CrossRef](#)] [[PubMed](#)]
25. Mazaheri, M.; Akhavan, O.; Simchi, A. Flexible bactericidal graphene oxide–chitosan layers for stem cell proliferation. *Appl. Surf. Sci.* **2014**, *301*, 456–462. [[CrossRef](#)]
26. Ku, S.H.; Park, C.B. Myoblast differentiation on graphene oxide. *Biomaterials* **2013**, *34*, 2017–2023. [[CrossRef](#)]
27. Liu, Y.; Luo, Y.; Wu, J.; Wang, Y.; Yang, X.; Yang, R.; Wang, B.; Yang, J.; Zhang, N. Graphene oxide can induce in vitro and in vivo mutagenesis. *Sci. Rep.* **2013**, *3*, 3469. [[CrossRef](#)]
28. Salesa, B.; Llorens-Gómez, M.; Serrano-Aroca, Á. Study of 1D and 2D Carbon Nanomaterial in Alginate Films. *Nanomaterials* **2020**, *10*, 206. [[CrossRef](#)]
29. Wick, P.; Louw-Gaume, A.E.; Kucki, M.; Krug, H.F.; Kostarelos, K.; Fadeel, B.; Dawson, K.A.; Salvati, A.; Vázquez, E.; Ballerini, L.; et al. Classification Framework for Graphene-Based Materials. *Angew. Chem. Int. Ed.* **2014**, *53*, 7714–7718. [[CrossRef](#)]
30. De Oliveira, P.V.; Zanella, I.; Bulhões, L.O.S.; Fagan, S.B. Adsorption of 17 β - estradiol in graphene oxide through the competing methanol co-solvent: Experimental and computational analysis. *J. Mol. Liq.* **2021**, *321*, 114738. [[CrossRef](#)]
31. Aguilar, T.; Sani, E.; Mercatelli, L.; Carrillo-Berdugo, I.; Torres, E.; Navas, J. Exfoliated graphene oxide-based nanofluids with enhanced thermal and optical properties for solar collectors in concentrating solar power. *J. Mol. Liq.* **2020**, *306*, 112862. [[CrossRef](#)]
32. Afaq, F.; Mukhtar, H. Effects of solar radiation on cutaneous detoxification pathways. *J. Photochem. Photobiol. B Biol.* **2001**, *63*, 61–69. [[CrossRef](#)]
33. Song, X.; Mosby, N.; Yang, J.; Xu, A.; Abdel-Malek, Z.; Kadekaro, A.L. α -MSH activates immediate defense responses to UV-induced oxidative stress in human melanocytes. *Pigment. Cell Melanoma Res.* **2009**, *22*, 809–818. [[CrossRef](#)]
34. Panich, U.; Tangsupa-A-Nan, V.; Onkoksoong, T.; Kongtaphan, K.; Kasetsinsombat, K.; Akarasereenont, P.; Wongkajornsilp, A. Inhibition of UVA-mediated melanogenesis by ascorbic acid through modulation of antioxidant defense and nitric oxide system. *Arch. Pharmacol. Res.* **2011**, *34*, 811–820. [[CrossRef](#)]
35. Pluemsamran, T.; Onkoksoong, T.; Panich, U. Caffeic Acid and Ferulic Acid Inhibit UVA-Induced Matrix Metalloproteinase-1 through Regulation of Antioxidant Defense System in Keratinocyte HaCaT Cells. *Photochem. Photobiol.* **2012**, *88*, 961–968. [[CrossRef](#)]
36. Duan, D.; Derynck, R. Transforming growth factor- β (TGF- β)-induced up-regulation of TGF- β receptors at the cell surface amplifies the TGF- β response. *J. Biol. Chem.* **2019**, *294*, 8490–8504. [[CrossRef](#)]
37. Erlebacher, A.; Filvaroff, E.H.; Ye, J.-Q.; Derynck, R. Osteoblastic Responses to TGF- β during Bone Remodeling. *Mol. Biol. Cell* **1998**, *9*, 1903–1918. [[CrossRef](#)]
38. Kuczyk, M.A.; Steffens, S.; Schrader, A.J.; Vetter, G.; Eggers, H.; Blasig, H.; Becker, J.; Serth, J. Fibronectin 1 protein expression in clear cell renal cell carcinoma. *Oncol. Lett.* **2012**, *3*, 787–790. [[CrossRef](#)]
39. Seyedin, S.M.; Thomas, T.C.; Thompson, A.Y.; Rosen, D.M.; Piez, K.A. Purification and characterization of two cartilage-inducing factors from bovine demineralized bone. *Proc. Natl. Acad. Sci. USA* **1985**, *82*, 2267–2271. [[CrossRef](#)]
40. Danen, E.H.; Yamada, K.M. Fibronectin, integrins, and growth control. *J. Cell. Physiol.* **2001**, *189*, 1–13. [[CrossRef](#)]
41. West, J.J.; Harris, T.J.C. Cadherin Trafficking for Tissue Morphogenesis: Control and Consequences. *Traffic* **2016**, *17*, 1233–1243. [[CrossRef](#)]
42. Nelson, A.R.; Fingleton, B.; Rothenberg, M.L.; Matrisian, L.M. Matrix Metalloproteinases: Biologic Activity and Clinical Implications. *J. Clin. Oncol.* **2000**, *18*, 1135. [[CrossRef](#)] [[PubMed](#)]
43. Zhang, X.; Yin, J.; Peng, C.; Hu, W.; Zhu, Z.; Li, W.; Fan, C.; Huang, Q. Distribution and biocompatibility studies of graphene oxide in mice after intravenous administration. *Carbon* **2011**, *49*, 986–995. [[CrossRef](#)]